Available online at www.sciencedirect.com
SCIENCE DIRECT®
Carbohydrate Research 340 (2005) 943–958
Carbohydrate RESEARCH

The disordered conformation of κ-carrageenan in solution as determined by NMR experiments and molecular modeling

Marco Bosco,[a,†] Annalaura Segre,[b] Stanislav Miertus,[a,‡] Attilio Cesàro[c] and Sergio Paoletti[c,*]

[a]*POLY-biós Research Center, AREA Science Park, Padriciano 99, I-34012 Trieste, Italy*
[b]*Istituto di Metodologie Chimiche, CNR Area della Ricerca di Roma, via Salaria km. 29.300, I-00016 Monterotondo Scalo, Italy*
[c]*Dipartimento di Biochimica, Biofisica e Chimica delle Macromolecole, Università di Trieste, via L.Giorgieri 1, I-34127 Trieste, Italy*

Received 23 September 2004; accepted 23 January 2005

Dedicated to Professor David A. Brant

Abstract—The conformation of κ-carrageenan in solution was studied combining ^{1}H and ^{13}C NMR with molecular mechanics. The experimental conditions were chosen to characterize the disordered conformation of the polymer. Particular attention has been given to explore a wide range of experimental conditions as to the dependence on solvent (water and Me_2SO), polymer concentration, temperature, pH, presence of a denaturing agent (guanidinium chloride), and of ions otherwise able to induce conformational order of the carrageenan chains, either in solution (I^-) or in the gel state (Rb^+). Two-dimensional NOE experiments were analyzed to obtain information on internuclear distances, and molecular mechanics provided the range of energetically accessible conformations. Two inter-residue topological constraints were clearly identified: their combination is rather restricting for the chain and suggests that the disordered conformation of κ-carrageenan is characterized by an intrinsic stiffness with high values of persistent length and characteristic ratio. They also rule out any postulated interchain hydrogen bonds. In contrast, experiments on the temperature dependence of the chemical shift in Me_2SO reveal the existence of two inter-residue intramolecular H-bonds which might contribute positively to the rigidity of the polymer chain. The overall picture emerging from the present results is that of a locally elongated 'loose single helix'.

Keywords: Carrageenan; Structure; NMR; NOESY; Molecular modeling; Conformation

1. Introduction

Advanced NMR methods,[1] coupled with the powerful computational tools of molecular modeling, have brought an impressive contribution to the structural elucidation of biopolymers. The latter method, soon after its application to proteins and nucleic acids, was extended also to polysaccharides with the pioneering work of Brant.[2] Advanced NMR investigations of proteins and nucleic acids have received most of the attention so far, whereas, because of limited solubility and overcrowded spectra, polysaccharides have received little benefit from such powerful technology.[3] Aiming to contribute along this line, we undertook a combined NMR and molecular modeling investigation of the algal ionic polysaccharide κ-carrageenan. Its idealized primary structure is that of a regularly alternating copolymer of D-galactose 4-sulfate (hereafter: S), β-(1→4) linked to 3,6-anhydro-D-galactose (hereafter: A) whose anomeric carbon is α-linked to position 3 of the (4-sulfate)-galactose comonomer S (Fig. 1). Under proper physicochemical conditions, κ-carrageenan gives rise to thermoreversible gels:[4] that is, gels are formed at low temperature, high ionic strength, high polymer concentration and, notably, in the presence of alkali-metal counterions of high ionic radius (K^+, Rb^+, Cs^+), while

* Corresponding author. E-mail: paolese@bbcm.univ.trieste.it
† Present address: Caffaro S.p.A. Divisione Ricerca, P.le F. Marinotti, 1, 33050 Torviscosa, Italy.
‡ Present address: ICS-UNIDO, AREA Science Park, Padriciano 99, 34012 Trieste, Italy.

0008-6215/$ - see front matter © 2005 Elsevier Ltd. All rights reserved.
doi:10.1016/j.carres.2005.01.035

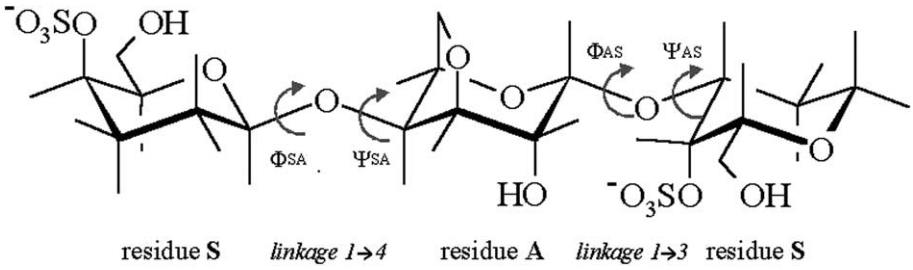

Figure 1. Idealized primary structure of κ-carrageenan segment with regularly alternating comonomers of D-galactose 4-sulfate (**S**) and 3,6-anhydro-D-galactose (**A**).

highly solvated ions such as Li^+, Na^+ have a much less favorable effect on gel formation. Another interesting feature of κ-carrageenan is its ability to produce (nematic) mesophases at suitable polymer concentrations of its Na^+ salt form in the presence of I^- anions.[5] This behavior has been consistently explained in terms of a significant elongation and stiffness of the carrageenan chain.[6]

Besides being one of the algal polysaccharides of great industrial importance, κ-carrageenan has given rise to one of the most intense debates on secondary structure in the whole field of polysaccharides.[7–23] Rees and coworkers have brilliantly associated the gelation process to that of a disorder-to-order conformational transition, as monitored by an increase of the optical rotation.[7,11,12] Conflicting opinions arise as to the topology of the fundamental ordered structure in solution. The competing models are a coaxially intertwined double-helix[7,11,12,16,17,20] and a single-strand helix.[8,9,13–15,18,21–23]

A contribution to understanding the molecular mechanism of formation of thermoreversible gels can be derived from study of the structurally related polysaccharide agarose. Convergent evidence from X-ray diffraction[24] and small-angle neutron scattering[25,26] has indicated that '*gelation*[of agarose] *occurs because of the existence of stiff chains*',[27] in view of the comparatively high persistence length (about 7 nm) even in the so-called 'conformationally disordered' state of agarose. Such a disordered conformation should be looked upon as a 'loose helix', that is '*a near-helical structure for which atomic position correlations vanish rapidly compared with those for a tight helix. On lowering the temperature, the loose helices should merely transform into tight helices and then align*'[27] thus giving rise to the junctions of the gel structure. It also seemed useful not to dismiss the concept of a 'loose helix' in the study of κ-carrageenan conformation, owing to the afore-said structural similarities and to the known stiffness of κ-carrageenan (a value of the persistence length in conditions of infinite ionic strength of 6.8 nm has been indicated on the basis of light-scattering results[18]).

NMR work has not yet unveiled by NOESY experiments the detailed conformation of the κ-carrageenan polymer in dilute solution. The wealth of NMR data and interpretations (largely limited to oligomers) has been essentially confined to elucidation of the chemical structure,[28–35] making it possible, in some cases, to estimate gross conformational effects in non-aqueous solvents, or the physicochemical features of the interaction with cations[36,37] and anions.[9,38] To the best of our knowledge, there are only a few reports on NOESY experiments relevant for κ-carrageenan, and these are confined to disaccharides.[39–41]

The present study employs a combined NMR/molecular modeling strategy, and is not centered only on molecular modeling with those results considered as instrumental for a better understanding of the experimental data on the polymer. The experimental NMR work is focused initially on the major intrinsic conformational features of the chain in dilute solution and the related backbone stiffness, followed by a detailed analysis of the H-bonding pattern. When expedient, counterions and co-ions have been used to specifically produce incipient conditions of chain ordering, eventually resulting in the presence of either a highly viscous solution (with I^-) or of a gel (with Rb^+). Study of the ordered conformation of κ-carrageenan and of its association behavior in the 3-D gel matrix per se is not the purpose of this paper. It was chosen to carefully investigate a range of conditions to afford sound information on the geometrical and macromolecular constraints for use in with the molecular-modeling analysis, providing a solid background for identifying in further studies the fundamental ordered conformation in dilute solution.

2. Materials and methods

2.1. Polymer sample

All experiments used a commercial sample of κ-carrageenan (from *Eucheuma cottonii*, Sigma Chem. Co., lot 19F0637), and the polymeric material was purified from low-molecular weight fractions and from gel-forming cations. κ-Carrageenan (750 mg) was dissolved in 50 mL of distilled water and the solution was then added to 150 mL of 70% EtOH–water containing 1.5% (w/v) of Me_4NCl. After adding 50 mL more of pure EtOH, the

resulting gel-like heterogeneous system was stored for 15 min at 4 °C. The polymer was then squeezed and washed twice with 70:30 EtOH–water and finally with pure EtOH. The sample was then dissolved in 70 mL of distilled water and kept for 1 h at 70 °C under stirring. Me_4NCl (8.2 g) was then added portionwise, corresponding to a 50 times excess of salt to κ-carrageenan. The solution was dialyzed against distilled water for seven days, filtered through Millipore filter (0.45 μm) and freeze-dried. Unless otherwise stated, in all experiments the Me_4N^+ form of κ-carrageenan was used, whose repeating unit was assumed to have an equivalent weight of 459 g mol^{-1}. GPC-LALLS experiments used the experimental procedure described already,[42] based on the use of a LALLS detector (Chromatix CMX-100) and two serial columns (TSK G6000PW and G5000PW, Tojo Soda Inc.), have given $\overline{M}_w = 3.3 \times 10^5$ and $\overline{M}_n = 1.43 \times 10^5$, respectively ($DP_n \approx 310$).

Atomic absorption measurements were performed to detect residual presence of K^+ cations; the residual concentration of K^+ corresponded to a molar ratio 1:230 to the polymer repeating unit (i.e., 0.04% w/w), whereas the Na^+ contamination was equivalent to a molar ratio 1:27 (0.19% w/w). The amount of Mg^{2+} corresponded to a 1:154 molar ratio (0.03% w/w). It is noteworthy that divalent cations do not seem to significantly affect the conformation of κ-carrageenan. To support this observation, increasing amounts of $CaCl_2$ were added to the κ-carrageenan solution, but no variation of the chemical shift nor of the line width in the ^1H NMR spectra of the polymer was detected up to a metal-to-polymer molar ratio of 20:1. The minor contamination from divalent cations was then assumed to have no further bearing on the conformational properties of κ-carrageenan.

The ^{13}C NMR spectrum of κ-carrageenan in the Me_4N^+ form shows a small peak at 92.1 ppm attributable to an ι-carrageenan (the doubly charged analog of κ-carrageenan) impurity whose intensity corresponds to ~2.5% (mol) in comparison to the signals of κ-carrageenan, as confirmed by integration of the corresponding signals in the ^1H NMR spectrum. This sample of κ-carrageenan appears to be one of the purest so far reported.

A κ-carrageenan fraction of lower MW was obtained by storing a polymer solution at room temperature in acidic conditions (pH = 2.8) for one week. The resulting material (with a $DP_n \geqslant 40$, estimated by NMR) gave a much better resolved ^1H NMR spectrum, allowing full assignment of chemical shifts and coupling constants. The NMR experiments confirmed that the mild conditions of hydrolysis did not produce any structural change.

In all experiments, Me_4NCl and Me_4NI, RbCl, and guanidinium chloride were P.A. commercial reagents from Fluka.

2.1.1. Preparation of solutions. Since aggregation often causes difficulties in the interpretation of the experimental data on κ-carrageenan, the present study avoided conditions, which could produce aggregation. The thermal and physicochemical history of the sample was carefully controlled as insufficient time and temperature allowed in the redissolution of a freeze-dried sample produces a long-lasting presence of (metastable) associated chains, which is very difficult to eliminate.[18,21–23] The presence of gelling counterions, such as K^+, Rb^+, or Cs^+, the polymer molecular weight and concentration, the physical state of the solid polymer, the temperature and the ionic strength of the solvent are all factors able to change the state of the polymer in solution. To study the polymer in its non-associated conformation, high values of polymer concentration and ionic strength were carefully avoided even with non-gelling cations. In particular, the polymer was never freeze-dried nor precipitated from aqueous solution unless followed by extensive rehydration and high-temperature conditioning.

For the study of the gel form, solutions containing Rb^+ cations were always added to a molecularly disperse solution of polymer in its non-gelling form at high temperature: homogeneity was additionally ensured by repeated cycles of heating and cooling.

2.1.2. Optical measurements. The specific rotations of water solutions of κ-carrageenan in the Me_4N^+ form, at a concentration of 5 mg mL^{-1}, were measured at $\lambda = 365$ nm, using a Perkin–Elmer 241 spectropolarimeter and a water-jacketed thermostatted cell.

2.1.3. NMR spectroscopy. All ^1H and ^{13}C NMR spectra were measured on a Bruker AMX 600 spectrometer. In a preliminary scanning of operating conditions, ^1H NMR spectra did not show any difference in the polymer concentration range from 0.25 mg mL^{-1} up to 13 mg mL^{-1}. Unless otherwise stated, all ^1H measurements employed samples having a concentration of 5 mg mL^{-1}. A concentration of 13 mg mL^{-1} was used for the ^{13}C NMR spectra.

All 2D experiments were performed in the phase-sensitive mode using TPPI.[43] 2D NOESY[44] spectra were obtained at different temperatures for κ-carrageenan Me_4N^+ form in D_2O solution and also in Me_2SO-d_6 solution. All 2D NOESY experiments were measured with a 30 ms mixing time. Two-dimensional spectra were stored with 512×256 data points and processed, after zero filling in F1, with a Gaussian window multiplication before the Fourier transformation. For both solutions ^1H NMR spectral assignments were made with a 2D COSY45 experiment.[45] Some experiments were also made on solutions in Me_2SO-d_6 containing 1 M guanidinium chloride as the denaturing agent; for these experiments, mono-dimensional and bi-dimensional

spectra were performed using solvent presaturation sequences with the carrier frequency on the guanidinium signal at 7.2 ppm. A 2D TROESY[46] spectrum was obtained at 333 K using a 5 kHz spin-lock power. $^{13}C\{^1H\}$ NMR spectra of κ-carrageenan in D_2O solution were measured at 303, 323, and 343 K.

The interaction of Rb^+ with the polysaccharide was studied on a 5 mg mL^{-1} κ-carrageenan solution in the presence of 50 mM aqueous RbCl. ^1H NMR spectra were obtained every five degrees in the range 303–363 K; at 343 and 363 K 2D NOESY spectra were also recorded, on the same solution.

Selective 1D versions of NOESY,[47] ROESY and TROESY experiments were performed by means of a selective spin-echo pulse sequence. The selective excitation was obtained by means of a DANTE train ($\pi/2$) followed by a second DANTE train (π) followed by a proper delay; in this way a DANTE echo is realized.[48] In these experiments the selective excitation was followed by the appropriate sequence, respectively, for NOESY, ROESY[49] or TROESY. Each component of the DANTE echo train was adjusted according to the needed selectivity. All pulses inside any sequence were obtained from the transmitter in the low-power mode, with an internal attenuation variable from 12 to 17 dB, according to the desired power level. With these conditions, the $\pi/2$ flip angle is obtained with a 30–50 μs pulse. This pulse is sufficiently strong to excite homogeneously the entire spectral width and is long enough to produce selective excitation by means of the DANTE trains. This compromise is sufficient to avoid any phase shift between the selective and the hard pulses, which might arise from any change in the power level. Optimal values for the short pulses in the DANTE train were about 1 μs. We overcame imperfect leading edges of the transmitter by substituting the elementary 1 μs pulse with two pulses of 3.5 and 2.5 μs, respectively, with opposite phases; a delay of 3 μs between the two pulses is called for the phase switch. This modification does not substantially increase the total pulse length: on the contrary it provides effective rectangular pulses with an equivalent length of few tenths of a microsecond. Typical values for the $\pi/2$ DANTE pulse were 50 repetitions of the loop with a 240 μs delay. The π pulse of the selective echo was also performed with the same modification of the DANTE scheme; moreover the delay was bisected (120 μs) in order to obtain the same length as for the $\pi/2$ component. This does not affect the selectivity, but strongly reduces the total length of the echo. The main advantage of the whole procedure is that leading edges of the transmitter pulse do not play any role. In the 1D NOESY sequence, a 2 ms trim pulse was introduced just after the reading pulse, to clear the dispersion components of the residual HOD signal which produces strong baseline distortions. No consequence of this trim pulse was detectable on any other signal. The residual water resonance was saturated with a 2.5 s low-power continuous-wave irradiation.

NMR studies were also performed in the presence of I^- anions using κ-carrageenan solutions in D_2O in the presence of 0.20 M Me_4NI. As reported in the literature, under such conditions a thermally reversible conformational transition takes place,[18] albeit not devoid of some intermolecular association.[22] The temperature dependence of ^1H NMR spectra was studied in the range 303–363 K, while the structure was again investigated by 2D NOESY spectra at 328 K.

The HSQC-NOESY experiment was performed at 333 K and a low-molecular weight κ-carrageenan sample in D_2O was used to avoid spin-diffusion effects during the NOESY mixing time. The result was stored with 256×128 data points and processed with zero-filling in both dimensions using linear prediction in F1. A standard GE-HSQCNOESY pulse sequence was used; the NOESY mixing time was set to 75 ms and the relaxation time was set to 2.5 s.

2.1.4. Molecular modeling. Molecular mechanics calculations were used to prepare Ramachandran-like conformational energy maps with the fully unrestrained energy minimization procedure by using the CVFF force field[50] of the Insight II BIOSYM software package. Quasi-adiabatic conformational energy maps for the disaccharide were prepared by identifying the lowest energy structure at each (Φ,Ψ) point through minimization of the energy associated with all the other internal degrees of freedom.

Although the 3,6-anhydro bridge in the **A** residue significantly reduces the degree of freedom, the number of possible states for the tetrasaccharide is extremely large. To minimize all of these possible conformational substates for each (Φ,Ψ) point on the energy map, an approximate search procedure was adopted. This procedure involved constructing the map in several stages, starting with a simple approximation obtained by rotating the starting conformation rigidly about the glycosidic linkage torsions to points spaced on a regular $20° \times 20°$ grid in the (Φ,Ψ) space, followed by conjugate gradient minimization to convergence. Presumably some other low-energy structures would exist with different side-group orientations, but this method nonetheless identifies well the regions of the glycosidic linkage conformations generally excluded by steric clashes, and provides for the geometrical relationships necessary for the comparison with the NMR data.

Conformational energy maps have been calculated for the central, β-(1→4), S–A linkage in the A–**S**–**A**–S tetramer, as well as for the central, α-(1→3), A–S linkage in the S–**A**–**S**–A tetramer (the central residues are shown in Fig. 1). The glycosidic dihedral torsion angles are defined as in Ref. 51 following the older (although widespread) convention that the 0° corresponds to the *eclipsed* ('*cis*') position of H atoms linked to the C atoms

involved in the glycosidic linkage. Since the recent recommendations of IUPAC are different, all the explicit definitions and conversions are given:

- for the α-(1→3) linkage in the –**A**–**S**– unit:

$$\Phi_K = \text{K(A)–C-1(A)–O–C-3(S)}, \quad \text{with K} = \text{H-1, O-5 or C-2} \tag{1a}$$

$$\Psi_K = \text{C-1(A)–O–C-3(S)–K(S)}, \quad \text{with K} = \text{H-3, C-4 or C-2} \tag{1b}$$

The approximate conversion is

$$\Phi_H = \Phi_{O5} - 120^\circ = \Phi_{C2} - 120^\circ \tag{2a}$$

$$\Psi_H = \Psi_{C4} - 120^\circ = \Psi_{C2} + 120^\circ \tag{2b}$$

- for the β-(1→4) linkage in the –**S**–**A**– unit is

$$\Phi_K = \text{K(S)–C-1(S)–O–C-4(A)}, \quad \text{with K} = \text{H-1, O-5 or C-2} \tag{3a}$$

$$\Psi_K = \text{C-1(S)–O–C-4(A)–K(A)}, \quad \text{with K} = \text{H-4, C-5 or C-3} \tag{3b}$$

whose approximate conversion is

$$\Phi_H = \Phi_{O5} + 120^\circ = \Phi_{C2} - 120^\circ \tag{4a}$$

$$\Psi_H = \Psi_{C5} - 120^\circ = \Psi_{C3} + 120^\circ \tag{4b}$$

For sake of simplicity, the following notations will be used in the text:

$$\Psi_{SA} \equiv (\Psi_H)_{SA}, \quad \Phi_{SA} \equiv (\Phi_H)_{SA}, \text{ and}$$
$$\Psi_{AS} \equiv (\Psi_H)_{AS}, \quad \Phi_{AS} \equiv (\Phi_H)_{AS}$$

3. Results and discussion

3.1. Optical activity

The optical activities of a salt-free aqueous solution of κ-carrageenan, Me_4N^+ form, were measured as a function of temperature. The data (Fig. 2) of both the absolute value of the molar optical rotation $[\alpha]_{365}$ and its linear temperature dependence are in agreement with the previously reported data.[38] In particular, the non-sigmoidal decrease of [α] with increasing temperature shows that there is no evidence of ordered conformation in salt-free conditions at low temperature. Thus, the conformational behavior of the sample used is consistent with that previously described.[38] Moreover, the use of the procedure just described for the purification and solution preparation ensured that there was no aggregation or any other supramolecular assemblies, usually detectable as an anomaly of the optical activity.[15] The observed comparatively high value of [α], even in a supposed disordered conformation, and the linear decrease of [α] with increasing temperature is discussed later in relation to solution conformation.

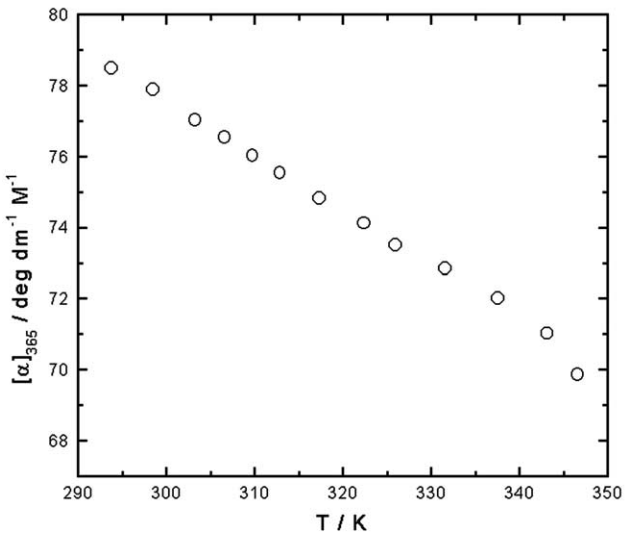

Figure 2. Temperature dependence of the optical rotation of κ-carrageenan (Me_4N^+ salt form, $c = 5$ mg mL^{-1}) in salt-free aqueous solution.

3.2. ^{1}H and ^{13}C assignment, temperature and pH dependence of the NMR spectra

Full assignment of the ^{1}H NMR spectrum was obtained from a COSY experiment. The chemical-shift values, δ, referred to TSP both for ^{1}H resonance (measured at 363 K in D_2O and in Me_2SO, always without any added salt) and for ^{13}C resonance (measured at 343 K), are reported in Table 1. For all ^{1}H and ^{13}C signals, the temperature dependence of the δ values in the range 303–363 K is linear. The slopes, $d\delta/dT$ (expressed as ppb K^{-1}), obtained from linear regression analysis are also reported in Table 1.

Different temperature dependences were observed in the presence of both I^- and Rb^+: the relative values of the ^{1}H integral of A1 as a function of temperature show a sigmoidal decrease from 1 to 0. This decrease corresponds to line broadening that is associated to the disorder-to-order conformational transition.

In order to check the spectral stability upon changing other solution variables, ^{1}H NMR spectra of κ-carrageenan solutions were measured in the pH range 2.85–13.8: within this pH range identical spectra were obtained.

Table 1. Relevant NMR parameters of indicated atoms of κ-carrageenan

	δ^1H_{DMSO}	$^3J_{HH}$	dδ/dT	$\delta^1H_{D_2O}$	dδ/dT	$\delta^{13}C_{D_2O}$	dδ/dT
A1	4.950	2.41	−0.27	5.100	−0.01	95.2	10.4
A2	3.812	4.2	−0.04	4.132	−0.11	69.6	3.6
A3	4.132	0.9	−0.12	4.512	−0.29	79.9	−2.4
A4	4.388	[a]	0.75	4.609	[b]	78.9	−0.9
A5	4.388	[a]	−0.97	4.630	[b]	76.8	1.9
A6a	3.860	[a]	−0.62	4.194	−0.50	69.6	3.6
A6b	3.795	[a]	[b]	4.054	−0.10	69.6	3.6
S1	4.307	7.7	−0.27	4.620	[b]	102.5	0
S2	3.273	9.3	0.61	3.603	0.19	69.9	5.3
S3	3.660	2.9	−0.23	3.952	−0.86	78.9	13.7
S4	4.489	1	0.07	4.819	−0.62	74.1	6.5
S5	3.494	6.4/5.8	−0.26	3.800	−0.06	74.8	−0.3
S6a	3.558	−10.9	0.72	3.790	[b]	61.3	−0.3
S6b	3.434	−10.9	0.25	3.810	[b]	61.3	−0.3

[a] Line width equal or larger then $^3J_{HH}$.
[b] Overlapping signals at lower temperatures.

3.3. NOE experiments

Very detailed structural information can be extracted from the NOESY experiments performed under different experimental conditions. They were performed in D_2O and Me_2SO-d_6, at several temperatures and (for D_2O) in the presence of different amounts of various 1:1 electrolytes. The fraction of ordered conformation, as determined from optical activity and/or decrease of ^1H signal intensity (data not shown), was found to be zero in all experiments except that carried out in the presence of I^- at 328 K (in D_2O). For the latter, the fraction of ordered conformation was estimated to be about 0.27 from the ^1H integral. Registration of signal intensity was equally possible for the experiments carried out in the presence of Rb^+ at 363 and 343 K (in D_2O).

All attempts at recording NMR spectra of κ-carrageenan in the fully ordered conformation either in solution (in the presence of I^- anions) or in the gel state (in the presence of Rb^+ cations) failed because of complete loss of the ^1H signal, which became broad and undetectable.

The most striking result from the NOESY spectra (see Fig. 3) was that some cross-peaks were observed between atoms for which internuclear distances are of the order of, or larger than, 5 Å, as calculated for the fully extended conformation of the polymer chain. These anomalous cross-peaks were present even under strong denaturing conditions (Me_2SO + 1 M guanidinium chloride, at 363 K), and the integral of these cross-peaks presented only an insignificant decrease upon increasing temperature. The cross-peaks were not detected in the experiments with the low molecular weight fraction of κ-carrageenan. Among these cross-peaks the strongest are those for A1-S5 and A1-S1 protons (Fig. 1). Although, at first instance, these cross-peaks might have been attributed to short distances between nuclei belonging to different chains and therefore ascribable to interchain interactions, it should also be recalled that interproton distances larger than 5 Å can also be observed in NOESY experiments in the presence of spin diffusion.[52] It is also known that the spin-diffu-

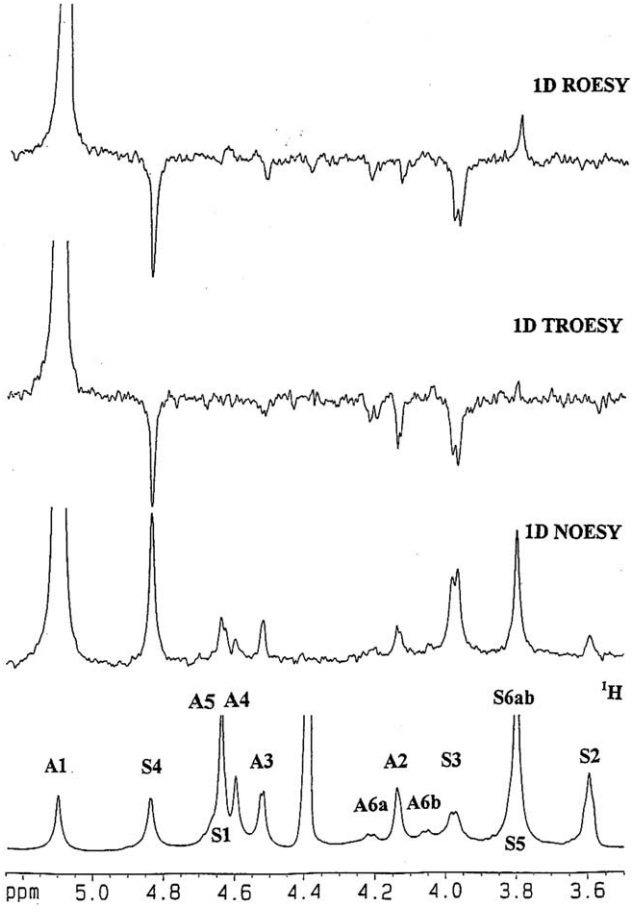

Figure 3. ^1H NMR spectrum of a 0.5% (w/v) solution of κ-carrageenan, Me_4N^+ salt form, in D_2O at 333 K. 1D NOESY, 1D ROESY, and 1D TROESY obtained after selective excitation of the anomeric proton (A1) of the 3,6 anhydro-D-galactose residue. For all the experiments the mixing time was 60 ms.

sion phenomenon is not present in small molecules with high values of reorientational correlation time, while it is very intense with high molecular weight, comparatively rigid polymers. Although all 2D NOESY spectra were obtained with a very short mixing time (30 ms), strong three-spin effects are still expected to be present in rigid molecules. Several polysaccharides are rather stiff molecules, with very limited segmental motion and quite long correlation time, depending on the glycosidic linkage.[53] In smaller molecules, three-spin effects produce positive cross-peaks in NOESY experiments, whereas the real direct contacts are negative with respect to the diagonal. Unfortunately, in the case of macromolecules, both true and three-spin contacts produce positive cross-peaks.

The foregoing considerations prompted us to undertake a more rigorous analysis of the NOE experiments to discriminate whether the cross-peaks originate from chain–chain interaction or from spin diffusion. In order to demonstrate both types of contacts, ROESY experiments may be used.[54] In fact, ROESY cross-peaks are negative for all τ_c values. In Figure 3 a selective 1D ROESY experiment is shown and is compared with the corresponding 1D NOESY spectrum, both performed with selective excitation on proton A1. In the ROESY experiment the strong cross-peaks with S5 and S1 are positive, thus clearly confirming their real nature of indirect contacts. Therefore, the magnetization of A1 is transferred to S5 through two intermediate nuclei (S3 and S4), which are close in space to both A1 and S5. On the other side, S1 can receive magnetization from A1 only through S3; since only one pathway of cross relaxation is allowed, its cross-peak is weaker than that of S5. It must also be noted that, in the $^4C_1$ pyranose chair conformation, S5 and S1 are 1,3 diaxial protons, as well as diaxial with respect to S3, and thus their distances are very short (about 2.5–2.6 Å).

To demonstrate the absence of artifacts and to increase, if necessary, the soundness of the conclusions on internuclear distances, a version of the ROESY pulse-sequence, called TROESY, was also used.[46] In TROESY, to avoid the evolution of undesired TOCSY components, the spin lock is obtained by a repetition of 180° pulses, spaced by a short delay. Figure 4 shows the 2D TROESY spectrum in which only direct contacts are present. No other contacts are present, either in D_2O or in Me_2SO solutions. From this experiment we can safely conclude that all observed cross-peaks can be explained in terms of a single chain, and that no evidence exists for the presence of a double-chain. Moreover, since the relative integrals of the cross-peaks are not much affected by temperature and by the nature of the solvent under the range of conditions investigated, it seems reasonable to conclude that the overall local conformation is not appreciably different under these circumstances.

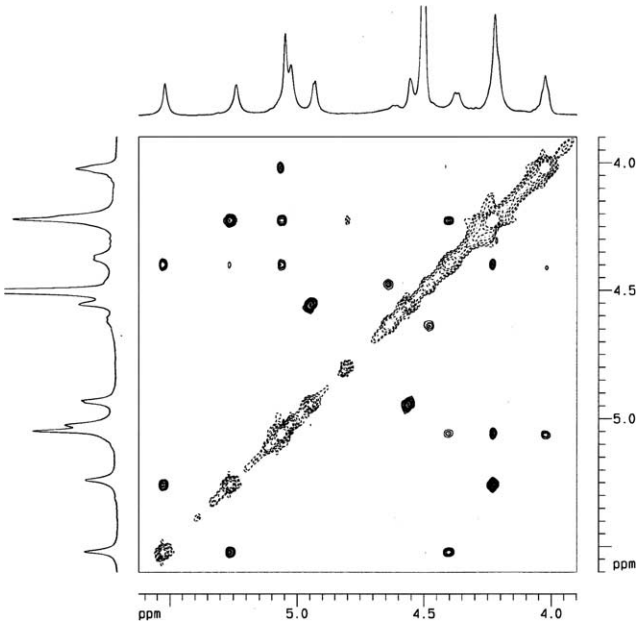

Figure 4. 2D TROESY spectrum of a 0.5% (w/v) solution of κ-carrageenan, Me_4N^+ salt form, in D_2O at 333 K. The mixing time was 30 ms.

From cross-peak intensities (I), the apparent internuclear distances r_{ij} can be determined by using the 'isolated spin pair approximation':[52]

$$r_A = (I_B/I_A)^{1/6} r_B \quad (5)$$

where I_B and r_B are the peak intensity and the distance of a reference pair of nuclei. In Table 2 the values of the internuclear distances are reported as obtained from the integrals of the cross-peaks. Since these data are obtained from two-dimensional spectra with limited digital resolution (5 Hz/pt), the estimated experimental error is about 10%.[55] In these calculations, the cross-peak S1–S3 was used as an internal reference (suffix B in Eq. 5); in fact this signal is well resolved in all experiments, and it is not affected by any scalar coupling. The value of r_{ij} for S1–S3 was set constant and equal to 2.65 Å, as an average between the value derived from the X-ray crystal structure (2.59 Å)[56] and the value (2.71 Å) currently obtained by molecular mechanics calculations. In any case the range of variation of the reference value of r_{ij} for S1–S3 is less than the estimated experimental error (10%).

The last column entry of Table 2 is the overall average value (±SD) for all available data for each pair of protons obtained under different conditions. The standard deviations of the average r_{ij} values reported in Table 2 are almost always smaller than the estimated error on the accuracy of the measurement: the average SD is 8.1%. It is noteworthy that the percent SD of the inter-residue interproton distances, which are very important as conformational constraints, are as low as 3.8%,

Table 2. Internuclear distances. r_{ij} (Å) from NOE data for κ-carrageenan

	Me_2SO salt-free	Me_2SO salt-free	D_2O salt-free	D_2O salt-free	D_2O salt-free ROE	D_2O salt-free	D_2O [I^-] 0.20 M	D_2O [Rb^+] 0.05 M	D_2O [Rb^+] 0.05 M	
T (K)	363	310	343	303	333	333	328	363	343	
PROTONS					r_{ij}/Å					$\langle r_{ij}\rangle$/Å
A1–A2	3.30[a]	3.22[a]	3.94[a]	3.68[a]	3.36[a]	[a]	[a]	[a]	[a]	3.50 ± 0.30
A1–A3	3.65	3.66	3.64	3.47	3.37	4.20	3.86	3.80	3.95	3.71 ± 0.25
A1–A6′	3.41	3.97	[b]	[b]	3.51	3.94	4.00	4.03	4.26	3.87 ± 0.30
S1–S5	2.62	2.77	2.52	2.28	2.53	2.89	2.78	2.77	2.71	2.65 ± 0.19
S3–S5	2.64	2.73	2.53	2.22	2.70	2.57	2.84	2.73	2.65	2.62 ± 0.18
A2–A3	2.49	2.42	2.27	2.01	2.10	[a]	2.61	2.64	2.47	2.38 ± 0.23
A3–A4	3.03	3.06	[b]	[b]	[b]	[b]	[b]	2.92	[b]	3.00 ± 0.06
S4–S5	2.72[a]	2.40[a]	2.34[a]	2.10[a]	2.14[a]	2.62[a]	2.61[a]	2.59[a]	2.52[a]	2.43 ± 0.23
S2–S4	4.11	4.38	3.92	3.52	4.5	[b]	[b]	4.88	4.61	4.27 ± 0.46
S3–A1	*2.51*	*2.74*	*2.58*	*2.74*	*2.48*	*2.70*	*2.75*	*2.65*	*2.66*	*2.65 ± 0.10*
S4–A1	*2.83*	*2.70*	*2.61*	*2.63*	*2.43*	*2.76*	*2.75*	*2.75*	*2.69*	*2.68 ± 0.12*
S2–S3	3.68	3.54	4.16	3.18	3.06	4.03[a]	3.81	[b]	4.50	3.75 ± 0.49
S4–A2	3.33	3.37	3.73	3.64	3.29	3.94	[b]	[b]	3.82	3.59 ± 0.26
S2–S1	3.91	3.95	[b]	[b]	2.69	[a]	3.54	[b]	[b]	3.52 ± 0.58

[a] Data affected by error due to scalar coupling ($^3J_{HH}$).[44]
[b] Cross-peak not found or overlapped with other resonance.

4.5%, and 5.6% for the proton couples S3–A1, S4–A1, and S4–A2, respectively.

Within the afore-mentioned limitations, the results show a similarity of the chain conformation under the different experimental conditions for which the optical data indicate the presence of a disordered conformation. This is true also for the salt-free aqueous solution over a temperature interval of 40 K, indicating that the modest linear increase of optical rotation on decreasing temperature corresponds to a progressive loss of disorder, albeit far from reaching complete helical stiffening. The data shown for the polymer in the presence of iodide ($[I^-]$ = 0.20 M at 328 K) are of particular interest. These conditions are in the range of the order–disorder conformational transition,[9] with about 27% loss of signal due to the conformational ordering. Under these circumstances, the residual, NMR detectable, disordered segments appear to show internuclear distances in very close agreement with those found for the other disordered conditions.

3.4. Local conformation accessibility

In order to capitalize the few but relevant geometrical constraints deduced from the NOE experiments, resort was made to Ramachandran maps of the carrageenan dimers, calculated according to the procedure described in the Materials and methods section.

Figure 5a shows the conformational energy map of the central α-(1→3) **A**–**S** linkage in the S–**A**–**S**–A tetramer, with an absolute minimum (AS-a) in the region around $\Phi_{AS} \approx -50°$ and $\Psi_{AS} \approx -10°$. Two local minima are also apparent: one (AS-b) is 1 kcal mol^{-1} above the absolute one and the other (AS-c) is at about 2.5 kcal mol^{-1} above AS-a, in agreement with our previous finding.[51] The relative difference of the energy of the minima and that of the separating barriers indicate the absolute minimum AS-a as the only relevant one in determining the conformational behavior of the A–S linkage.

The situation of the central β-(1→4) **S**–**A** linkage in the A–**S**–**A**–S tetramer is somewhat different. As is clear from Figure 5b, the β-(1→4) linkage is characterized by two large shallow minima, in the same range of $\Phi_{SA} \approx 40°$, one SA-a is in the broad region of Ψ_{SA} from 0° to −60°, while the other relative minimum SA-b lies in the region of Ψ_{SA} between 0° and +60°. A low-energy barrier separates these two minima (less than 1 kcal mol^{-1}). Moreover, the energy difference between the minima is only 0.41 kcal mol^{-1} in favor of SA-a. A third minimum SA-c with higher energy (2.5 kcal mol^{-1}) was also found in the range $\Phi_{SA} \approx +160°$ and $\Psi_{SA} \approx +40°$. Clearly, in this case the contribution from experiment is even more crucial than in the case of AS to resolve any possible ambiguity as to the preferred minimum.

However, it should be kept in mind that this work is mainly focused onto the NMR results and is principally aimed at shedding more light onto the *whole-chain* behavior of the κ-carrageenan polymer rather than on its constituent oligo- (or even di-)saccharides. We are well aware that, as of now, molecular modeling of the constituents may be an useful guide, but not the final answer for predicting such *whole-chain* behavior, unable as it is to tackle long-range effects and interactions, among which polyelectrolytic ones may be one of the most important. We are aware also of a severe limitation from the neglect of explicit consideration of the solvent in our calculations, and that some other force fields performed somewhat better with different low MW carbohydrates.[57] Still, the ultimate validity of any molecular

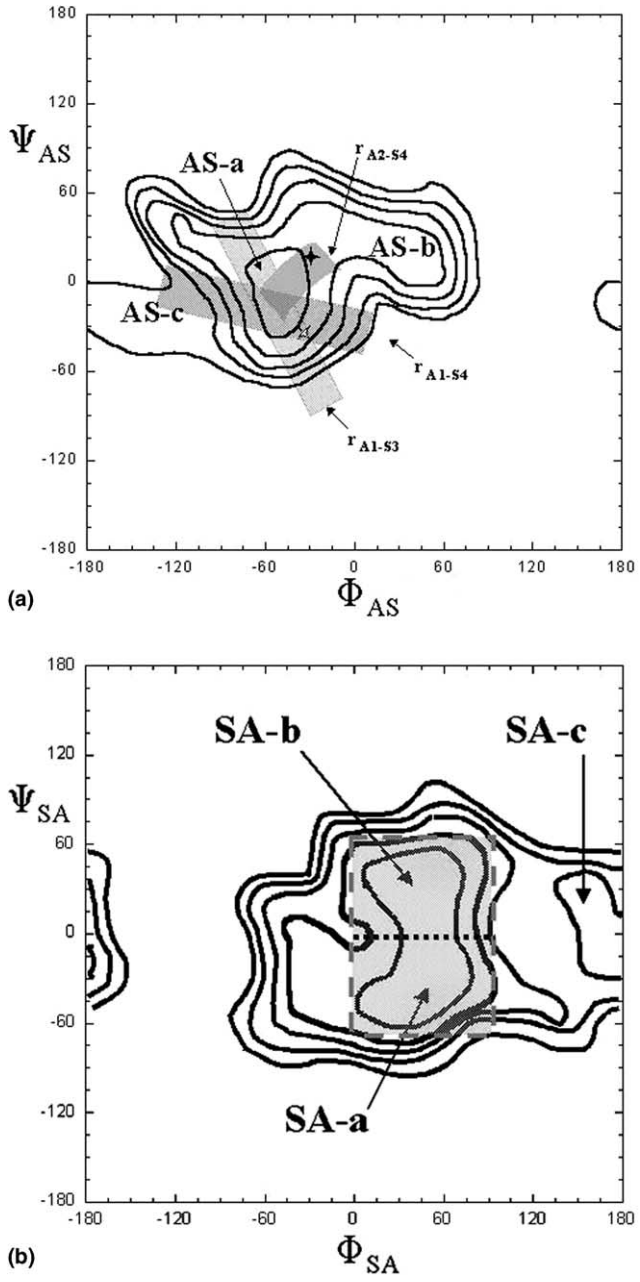

Figure 5. Conformational maps for the α-(1→3) (i.e., Φ_{AS}, Ψ_{AS}) (Fig. 5a) and β-(1→4) (i.e., Φ_{SA}, Ψ_{SA}) (Fig. 5b) glycosidic linkages, respectively. The maps were calculated for a tetrasaccharide using the CVFF force field with a dielectric constant $\varepsilon = 4$; contour lines were with an energy matrix of 19×19 minimized structures. The interval of energy contours was 1 kcal mol.

modeling tool resides in its ability to predict static and/or dynamic properties that agree with the experiment. This is the guideline for interpreting the following results.

3.5. Comparison of molecular modeling with NOE and with previous modeling results

The specific scope of this section is to use the NMR (NOE) constraint information described in the previous sections to delimitate as much as possible the range of accessible conformations found in molecular mechanics calculations of the dimeric units. A comparison between the present modeling results with other previous calculations from this laboratory[51] or from the literature[39–41,58–65] is made only with this spirit and not to rank the performance of the various modeling approaches. In passing, one may note that, although all the quoted papers deal with the conformational energy surfaces of algal galactan residues, it is necessary to keep in mind whether the results have been obtained on the sulfated dimeric units of carrageenan (A–S and S–A, respectively) and oligomers[40,41,51,58,63–65] or if they refer to the unsubstituted residues (neocarrabiose, A–G and carrabiose, G–A, respectively) and oligomers:[39,59–62] the two sets are likely to differ in some details. A thorough discussion of these results is outside the scope of this paper, and only the most relevant points are addressed. The reader is also alerted on the fact that the afore-mentioned papers used different definition of the glycosidic dihedral angles (see Fig. 1), as specifically illustrated in the Materials and methods section.

The presence of the two strong interglycosidic cross-peaks in the NOE spectra between A1–S3 and A1–S4, and a third weak contact between A2–S4 represents a powerful constraint for the theoretical description of the average conformation of the α-(1→3) glycosidic bond ('neocarrabiose 4′-sulfate'). In fact, at the center of the conformational map in the AS-a region, such a condition is fully met. Three different interproton distances can be used as NMR-derived constraints, namely, A1–S3 = 2.64 Å, A1–S4 = 2.68 Å and A2–S4 = 3.59 Å (see Table 2). Using consistent geometrical considerations, three curved stripes have been calculated and plotted in the conformational space in Figure 5a, corresponding to the distances r_{ij} given in Table 2 for atom pairs A-1–S-3, A-1–S-4 and A-2–S-4. The amplitude of the stripes encompasses a range of r_{ij} values to ±0.3 Å, corresponding to the estimated accuracy of the NOE derived distances. It may be seen that the overlapping part of the two stripes for S3–A1 and S4–A1 hits the region of the absolute minimum AS-a in its lower part, namely, at $\Phi_{AS} \approx -40°$ and $\Psi_{AS} \approx -20°$. Note that the A1–S4 distance is very sensitive to rotations related to the Ψ_{AS} dihedral angle, that would result into an increase of its average value up to a fading of the observed NOE. The internal consistency of the overlap region is also confirmed by the large value obtained for the A2–S4 distance (r_{ij} = 3.59 Å). Although the NMR distances are in principle averaged over all accessible conformations (and therefore may explore a range of torsional angles), this result is a clear indication of the very strong preference of the residue A–S to be essentially confined in the conformational basin identified as AS-a, which was indicated as the absolute minimum in the present calculations. The most recent work pertaining to this

linkage is that of Ueda et al.,[61] who reported the Ramachandran map of the conformational potential of mean force for neocarrabiose (unsulfated A–G) in water, obtained using molecular dynamics (MD) simulations with umbrella sampling to avoid inadequate statistics for the presence of multiple minima. The most significant result of that work is the identification of the global minimum in a region (called 'w') practically coinciding with our minimum AS-a, but different from the lowest minimum found using molecular dynamics in vacuo in a previous work of the same authors on the same system.[59] From molecular dynamics simulations (in water) the same authors reported[41] that the hydration water favored their well called 'a' (which is called 'w' in Ref. 61) and that their NOE–NMR data strongly indicated that the conformation in their 'a' well is the only stable one in water. The NOE results of Ref. 41 are in excellent agreement with ours, in this case pointing to a substantial similarity of the conformational behavior of the low-MW disaccharide and of the polymer in solution. This should not always be taken for granted. This global minimum largely corresponds to the minimum previously found by Urbani et al. (there called 'a_1', see Fig. 2a of Ref. 51) for both A–G and A–S by using molecular mechanics with refined structural and atomic parameters. A similar minimum ('C2') was identified by Lamba et al. (Fig. 4 of Ref. 39) by using MM2CARB in a study aimed at solving the molecular structure of neocarrabiose in the solid state and in solution. Molecular mechanics and molecular dynamics calculations—the latter with the presence of explicit water molecules and counterions—performed on neocarrabiose 2,4′-bis sulfate (the model disaccharide of ι-carrageenan) found that the most stable conformation corresponds almost exactly to our AS-a minimum.[63] Very similar results were obtained by Le Questel et al.,[58] who, however, used no electrostatic contribution. Finally, the position on the map of the minimum proposed on the basis of the fiber-diffraction data is marked by a cross (see Fig. 5a). It may be seen that the difference with the present NOE/modeling results is of about −10° only, both for Φ and for Ψ. Only the results by Stortz and Cerezo[65] markedly differ from the present ones, from all other reported calculations and from those of fiber diffraction. They ascribed their calculated excess energy (about 2.5 kcal mol^{-1}) for the conformation corresponding to the coordinates of the fiber diffraction analysis with respect to their minimum **A** to 'the presence of a tertiary structure, and [to] the fiber packing forces'.[65]

From the same type of experiments it is not possible to obtain equally detailed information as to the conformational preferences of the residue S–A (carrabiose 4′-sulfate). In fact, the contribution of the NOE constraints to a quantitative description of the S–A glycosidic bond is quite inaccurate, because in D_2O the signals A4 and S1 of the polymer are badly overlapped in the whole temperature range. However, in Me_2SO they are sufficiently resolved to allow detection of a strong cross-peak. Even if the integral of this cross-peak is affected by the proximity with the diagonal, this semi-quantitative information is still sufficient to predict a *cis*-like conformation (i.e., identifying an area between ±60° both for Φ_{SA} and Ψ_{SA}, around the central position $\Phi_{SA} = \Psi_{SA} = 0°$). This boundary condition clearly excludes conformations (such as SA-c) outside the central region; it corresponds roughly to the large shallow region including minima SA-a and SA-b (see Fig. 5b). However, the absence of other specific constraints does not permit straightforward identification of a well-defined sub-area within the large shallow minimum of regions SA-a and SA-b: all Ψ_{SA} values from roughly +60° to −60° bring proton A3 quite remote from S1.

To get more clear-cut information about the range of the preferred Φ_{SA} values, a HSQC-NOESY experiment was performed. The two most relevant results (not shown), albeit qualitative, strongly confirm the foregoing conclusions from data obtained in Me_2SO. The S1–A4 cross-peak in D_2O is clearly detected, whereas the S2–A4 cross-peak is absent; these two conditions rule out, once more, the possibility that basin SA-c is populated. Moreover, both the 2D NOESY and the HSQC-NOESY experiments clearly show no evidence for cross-peaks attributable to a short internuclear distance between protons S1 and A3, although their signals are well resolved in D_2O. The converging results indicate that the average distance, r_{ij}, must be larger than ≈4.5 Å (which would give an integral less than 5% of the reference integral).

At variance with these findings for the A–S dimer, significant difference is noteworthy between the present NOE results obtained on the polymer and those published by Parra et al.[40] In the case of carrabiose 4′-sulfate (κ-carrabiose) they observed *both* S1–A4 *and* S1–A3 interglycosidic cross-peaks, whereas in the polymer case, the S1–A3 one is definitely absent. (Note that the NOESY spectra for (nonsulfated) carrabiose and for carrabiose 4′,2-bis(sulfate) (ι-carrabiose) were not conclusive,[40] because of the overlapping of S1 and A4 resonances.) This corresponds to a non-negligible difference in the average conformation in solution, which in turn should reflect an energy preference for different conformational minima on the (Φ,Ψ) space. According to calculations reported by the authors[40] on the (desulfated) carrabiose analog, only the two minima called 'C2' and 'C3' produce distance values compatible with the NOE results: they are similar to both angular values ($\Phi_{C2} = -93°$, $\Phi_{C3} = -105°$, $\Psi_{C2} = 173°$, $\Psi_{C3} = 179°$) and energy ($E_{C2} = 0.00$, $E_{C3} = 0.13$ kcal mol^{-1}) so as to allow consideration of them as belonging to a single, wider energy well. The same seems to hold for the corresponding minima called 'KA1'&'KA2' in the work of Le Questel et al.[58] They correspond roughly to the large

minimum denoted as SA-b on our SA energy map. In accordance with the results of Parra et al., Stortz and Cerezo[65] stated that the NMR-determined conformation of κ-carrabiose in solution 'is closer to region **A**, predicted in the work [by Stortz and Cerezo], and not to region **B**, present in the fiber', in agreement also with previous results.[64] The recent work of Ueda et al.[63] investigated also the companion disaccharide carrabiose 4′,2-bis(sulfate). Although the global minimum conformation ('A1') corresponded to our minimum SA-a, the molecular-dynamics simulation in water suggested that the structure 'B1' (very close to C-2–C-3 of Parra et al.[40] and to **A** of Stortz,[64,65] corresponding to our SA-b) is more stable, by analyzing the trajectory and the hydrogen bonds with water molecules. The result was correctly interpreted as being corroborated by the NOE experiment of Parra et al.[40] However, it should not be overlooked that the modeling of Ueda et al. pertains to the repeating unit(s) of ι-carrageenan, in which the additional sulfate group is clearly shown to contribute to an increase of solvation with respect to κ-carrabiose.[63] Therefore, also on the basis of the calculations reported by Ueda et al.[63] (for minimum 'A1': S1–A4 distance = 2.38 Å and S1–A3 = 4.08 Å, 'a little too far to produce a NOE cross-peak'[63]) and the NOE results here presented for κ-carrageenan (which differ from those reported for κ-carrabiose[40]) it may be concluded that the polymer enchainment produces a conformational selection favoring the conformation corresponding to minimum SA-a, with respect to the disaccharide case where SA-b is likely to prevail. Interestingly, also the conformation of the SA linkage proposed on the basis of fiber-diffraction studies of ι-carrageenan polymer[7,17,62] falls within our SA-a region.

At this point, however, a word of caution is in order. The energy difference between our present minima SA-a and SA-b is very small (about 0.4 kcal mol^{-1}). A small energy difference also holds for the quoted calculations (Parra et al.[40] (0.892 kcal mol^{-1}—with an evident misprint from to 8.92 in their Table II—for 'C4' vs 'C2'&'C3'), Ueda et al.[63] (0.9 kcal mol^{-1} for 'A1' vs 'B1', with dielectric constant $\varepsilon = 80$ set to model water), Stortz[64,65] (0.9 kcal mol^{-1} for '**B**' vs '**A**')) as well as for the previous ones of Ueda et al.[60] (0.5–0.9 kcal mol^{-1} for 'b' vs 'c'&'d') and Le Questel et al.[58] (0.27 kcal mol^{-1} for 'KA3' vs 'KA1'&'KA2'). Moreover, the energy barrier between the two minima is not high.[63] Urbani et al.[51] even do not identify them as separate minima. Therefore, one should rather speak of 'a slight preference' for SA-a with respect to SA-b. Possible incursions from the former region into the latter one (or at least into part of it) are certainly possible, or even not probable. At the end of this part, the enlightening sentence by Stortz is appropriate:[64] '…the β linkage of carrageenans is more difficult to model than the α linkage, due to the larger number of low-lying conformations potentially accessible. The proximity in energy between the **A** and **B** regions in both cases makes it impossible to ascertain that either is predominant by just computer modeling. Subtle factors in the force-field parameterization may lead to wrong conclusions if these small energy differences are intended to make conclusive'.

3.6. Direct NMR study of hydroxyl protons in Me_2SO

Since the NOE pattern suggests that there is no significant difference between the average conformation in D_2O and that in Me_2SO, we tried to obtain the full body of information available from the NMR spectra in latter solvent. This is mostly useful in relation to the identification and localization of H-bonds. For κ-carrageenan, the temperature dependence of the chemical shift of skeletal protons is very modest both in D_2O and in Me_2SO. However, in Me_2SO between 303 and 358 K, hydroxyl protons give distinct resonances from which valuable information can be extracted. Because of proton exchange with residual water, their chemical shifts are very sensitive to temperature effect, and it normally follows the marked upfield drift of the water signal. Since the rate of the exchange between these protons and residual water increases with increasing temperature, at high temperature all hydroxyl group resonances should collapse within the water signal. Thus, in the absence of strong hydrogen bonds, an increase of temperature should be accompanied by a decrease of the chemical-shift difference between hydroxyl resonances and the water signal.[66]

In order to facilitate easier comparison among the hydroxyl signals, the chemical-shift difference from the water signal at temperature T, $\Delta_T = (\delta_{ROH} - \delta_{H_2O})_T$, is corrected for the corresponding value of Δ_T at 303 K, $\Delta_{303\ K}$. The values of $(\Delta_T - \Delta_{303\ K})$ as a function of T are reported in Figure 6 for hydroxyl protons OS2, OA2, and OS6. From this plot it may be seen that only OS2 follows the expected behavior. In contrast OA2 and OS6 show an opposite, albeit still linear, temperature dependence, that is, their frequency distance from the water resonance progressively increases. It must be emphasized that the linearity of the water shift (data not shown) ensures that no spurious effect is present. Hence these two OH groups must be involved in well-defined hydrogen bonds, in which both OA2 and OS6 are proton donors, the former one giving the strongest effect.

The hypothesis of hydrogen bonds involving these two hydroxyls was proposed on the basis of molecular-mechanics calculations and X-ray fiber diffraction data on the K^+ form of κ-carrageenan.[7] According to this model, the postulated hydrogen bond should be *inter*molecular, involving OA2 and OS6, and contribute to the stabilization of an intertwined double-helix.

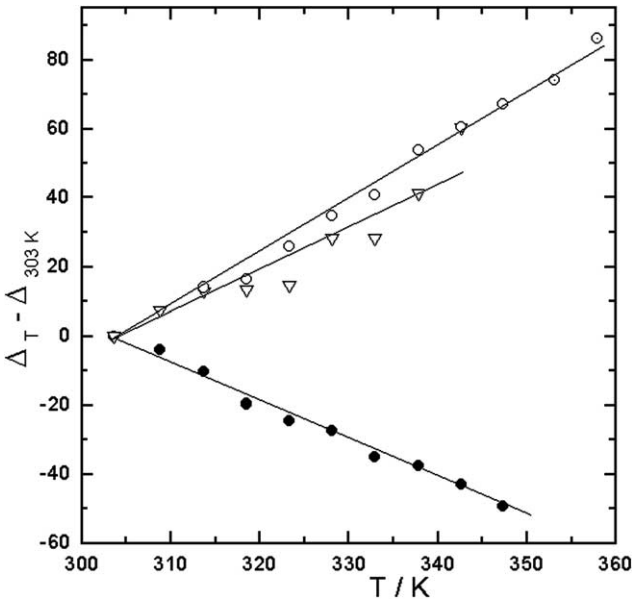

Figure 6. The difference of chemical shifts between each hydroxyl proton (○: OA2; ▽: OS6; ●: OS2) and the water signal in κ-carrageenan NMR spectra as a function of temperature. The comparison is relative to the resonance frequencies at 303 K.

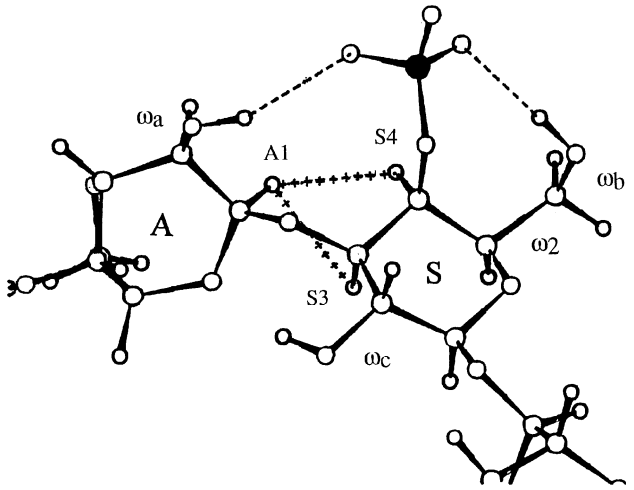

Figure 7. A representative structure ('snapshot') of the disaccharidic unit showing the relevant constraints revealed by COSY and the H-bond network suggested by hydroxyl resonances in Me_2SO. The dashed lines represent a 'bifurcated' hydrogen bond through a water-molecule bridging.

However, it has already been shown that in 2D NOESY spectra at 300 K it is not possible to detect any contact arising from either dipolar interaction or chemical exchange between the corresponding hydroxyl signals. Only cross-peaks between each OH signal and the signal of water are present, clearly due to the chemical exchange process. The hydrogen bonds involving OA2 and OS6 must then be *intra*molecular; the *inter*molecular H-bond, postulated for the double-helical conformation, does not exist in solution under a wide range of conditions.

Simple modelization (a snapshot is reported in Fig. 7) suggests that the corresponding hydroxyl groups (as donors) might well involve the S4 sulfate group as the common acceptor. The H bond lengths (2.3–2.7 Å) fall very nicely within the well-established range of bifurcated H-bonds, very common in carbohydrate structures.[67] This would imply the presence of one water molecule for each of the intramolecular H-bonds. The H-bond predictions of the convergent MD calculations of Ueda and Brady et al.,[41,61,§] are in excellent agreement with the NMR evidence obtained in Me_2SO, which points to the existence of two intramolecular H-bonds, involving OA2 and OS6 as hydrogen donors and sulfate (oxygens) as acceptor(s), through two bridging water molecules. A hydrogen bond between OA2 and one sulfate oxygen was clearly indicated also by the calculations of Stortz and Cerezo.[65] The situation in water lacks the direct support of NMR evidence as to the relative role of the hydroxyl groups. A similar detailed H-bond arrangement in water would still preserve essentially the same conformational and energetic pattern. For instance, inspection of the minimum conformation resulting from modeling reveals that OS6 could easily rotate to become exposed to a better interaction with the aqueous solvent, giving rise to an (at least partial) acceptor-like arrangement of OS6 with respect to H-atoms from solvent molecules. At the same time OS2 could fall at a reasonable distance (namely, between 3 and 4 Å) from OA2, thus allowing for the formation of another bifurcated intramolecular H-bond, still across the α-(1→3) glycosidic linkage. This possibility was clearly indicated by both the works of Ueda and of Brady et al.: the percentage of OA2–OS2 inter-residue water bridge ranged from 65%[41] to 83%.[61] It should anyway be added that a non-negligible fraction of trajectory time (ranging from about 20% to about 30%) was in both cases indicated for another inter-residue water bridge still involving H-atom of OS2, namely with the pyranosidic oxygen atom of the A ring (O-5 or O-5′, depending on the atom designation[41,61]). Also in this case, the OH group of the S residue would act as a proton donor, much like in the OS2–OA2 bridging. It should be emphasized that all of that would involve just a very small rotation of the set of (Φ_{AS},Ψ_{AS}) values. This is in agreement with the observation that NOE results point to practically the same accessible range of angles for the conformationally dis-

[§] Incidentally, the results of the present work were quoted as 'Submitted for publication' under reference numbers 32 and 55 in Ueda et al.[41] as 'Personal communication, 2001' under reference number 29 in Ueda et al.[61] and as reference number 35 in Bongaerts et al.[21]

ordered form of κ-carrageenan both in water and in Me_2SO.

The detailed molecular structure across the α-(1→3) linkage may be tentatively summarized as follows:

(i) two water-bridge-mediated H-bond arrangements run parallel to the glycosidic linkage, the former—'*major*'—connecting OA2 with OS6 through two *strong* bonds (see Fig. 7) at the central (highly electronegative) sulfate group, the latter *weak* bond arrangement—'*minor*'—connecting OS2 either to OA2 or to OA5 (ring oxygen). Both inter-residue enchainments would then significantly contribute to the polymer rigidity;
(ii) the OH residue OA2 involved in the '*major*' H-bond sequence is always an H-donor under all circumstances, due to the 'only-acceptor' nature of the sulfate oxygens;
(iii) the OH residue OS6 involved in the '*major*' H-bond sequence is clearly an H-donor in aprotic media (like Me_2SO: see Fig. 7) for the same reason as in (ii), but it can exert a more acceptor-like character when exposed to the aqueous solvent;
(iv) the OH residue OS2 involved in the '*minor*' H-bonds is always an H-donor: when to OA2, because of the 'always-donor' nature of OA2 to sulfate (see foregoing in (ii)), when to OA5 because of the trivial 'only-acceptor' nature of the ring oxygen.

Far from being a pedantic speculative exercise, the attribution of the donor/acceptor nature to the H-bonds must be looked upon as a stringent consequence of the H-bonding pattern at the α-(1→3) linkage, which can be subjected to experimental testing. In fact, one of us has recently proposed a new approach to assess the hydroxyl-group interactions in polysaccharides.[68] It is based on the deuterium-induced differential isotope shift (DIS) determined from ^{13}C NMR spectrum in aqueous solution. Deuterium substitution on positions β or γ with respect to a given carbon atom will cause an upfield (β effect) or downfield (γ effect) deuterium isotope-shift. DIS can be correlated with the involvement of a given C atom in H-bonding: low β-effect values are typically obtained when OH groups act as proton-donor entities in H-bonds; high β-effect values, such as those obtained in water hint at the presence of hydrogen bonds where solute OH groups are proton-acceptor systems. The meaning of *low* and *high* is relative to the set of values reported for a given C atom and linkage. Two cases can be identified in relation to the linkage type: the 1–4 and the 1–3 ones (numbering here refers to the positions involved in the two chain-linkages for a given sugar and NOT to sequence through the glycosidic linkage: to avoid confusion here we preferred to use the symbol '-' rather than '→'). Experiments were performed on coaxial setups, the polymer being dissolved both in H_2O and D_2O, at 333 K.[¶] The DIS value (ppb) for C-2 of α-(1→4) linked residue A of κ-carrageenan is 104. The DIS values (12 data values) for C-2 reported in Tables III and IV of Ref. 69 range from 104 (A in κ-carrageenan) to 122 (Rha in gellan), with two extreme cases at 141 (Glc) and 94 (GlcA), both in gellan. Except for Glc in pullulan (DIS = 100), the value of κ-carrageenan is lower than all other values. This unambiguously points to a donor nature of the OH group in OA2, as already predicted in point (ii). Coming to the β-(1→3)-linked residue S, the available data are for C-2 (OS2) and for C-6 (OS6). In a list of eight values, the DIS value of OS2 is 103, second lowest only to C2 of chondroitin 4-sulfate (102), all other values ranging from 105 to 119. Also, in this case, the identification of OS2 as a proton donor is straightforward, once more confirming the hypothesis above set out under (iv). In this respect, it should be clearly underlined that the donor/acceptor nature is not at all univocally correlated with the strength of a given H-bond, as demonstrated by the two preceding cases. Finally, the DIS value of C-6 (OS6) is 149: exactly in between the lowest reported value (142, for Glc in gellan, and for chondroitin 4-sulfate) and the highest one (154, for laminaran). It points to a bivalent role of OS6: partly as proton donor (toward the sulfate group, as in Me_2SO), partly as proton acceptor, from the wealth of water molecules that surround the highly electronegative region extending from C-4 to C-6 of galactose 4′-sulfate, again in accordance with what was written under point (iii). The agreement between the predictions for the α-(1→3) linkage based on the present NMR data (both NOE and temperature dependence of chemical shift in Me_2SO) and modeling, coupled with the extensive modeling work of Ueda and Brady, on one side, and the DIS ^{13}C NMR experimental results, on the other, are then very encouraging. It gives a rather solid base to start highlighting the molecular arrangement for this part of the carrageenan molecule.

Unfortunately, for the β-(1→4) linkage no such wealth of information is currently available. There is a clear need for more accurate modeling description and, hopefully, new advanced tools of investigation. Still, from the foregoing results one may tentatively derive a sound hypothesis to explain at the molecular level the temperature-induced conformational change of κ-carrageenan. The high-temperature conformation is already comparatively inflexible, with a rather loose network

[¶] Table VI of Ref. 68 also gives the DIS values for the κ-carrabiose disaccharide. This molecule is not considered further because it cannot help assessing the effect of the H-bond arrangement across the critical α-(1→3) linkage. Moreover, the 3,6-anhydrogalactose at the reducing end is predominantly in the open form, induced by ring conformational constraints. The proper model compound would be, for example, the methyl β-glycoside of neocarrabiose 4′-sulfate.

of H-bonds allowing for somewhat limited oscillations around the average position. On cooling, a cooperative 'freeze-out' of the α-(1→3) linkage conformation[8] will be accompanied by a tightening 'in register' of the intramolecular H-bond network. A similar cooperative 'freeze-out' of the β-(1→4) linkage conformation,[8] possibly involving the two conformational energy minima SA-a and SA-b, seems equally possible, although in this case no significant consequence on the H-bonding pattern is apparent from NMR data, nor from modeling. Both effects will contribute producing an even stiffer polymer, giving rise to long, ordered helical segments.

3.7. Statistical chain conformation

The combination of NMR constraints and molecular-mechanics calculations readily permits the modeling of the most stable helical structure. However, clearly stated in the Introduction, detailed analysis of the structure (including the topology) of the ordered conformation of κ-carrageenan is not within the scope of this work, and it will be reported in a forthcoming paper. Nonetheless, preliminary calculations point to a rather extended structure, with helical parameters close to those given in the literature for the single strand of the double-helix proposed for the solid state (right-handed 3_1 helix, with helix pitch = 24.6 Å).[7]

It is also apparent that, upon relaxing the minimum energy condition, the range of accessible conformations is still rather limited, under the constraints given by the NOE experiments. With respect to this point, the detailed study of the configurational statistics of the (disordered) κ-carrageenan chain of Urbani et al.[51] is relevant. For the S–A, residue their calculations produced two main distinct minima with very similar energy values. The one called b_1 (our present SA-c) corresponded to an angular range of Φ_{SA}, generating a folded structure, while the other conformation (b_2) (our present SA-a and SA-b) produced a rather extended structure. Such a result led the authors to consider all possible statistical frequency of the two conformers (namely, those corresponding to b_1 and b_2, respectively) in a Monte-Carlo calculation of the configurational statistics of the chain. They considered a model statistical chain made by $n = 100$ disaccharidic repeating units. The resulting characteristic ratio, C_n, showed, as a function of composition, the peculiar behavior of copolymeric structures. The chain dimension results were very low (C_n about 6, and persistence length, L_p, 1.8 nm) for a polymer with mixed conformational states in a wide compositional range around the ratio 50:50 of the two basins b_1 and b_2. The configurational statistics calculations of Le Questel et al. were based on the assumption of the '*existence of several low-energy conformers of which some* (*particularly GA* [i.e., SA in our present notation] *repeat*) *have comparable energies, and therefore comparable probabilities of occurrence*'.[58] The result predicts a '*high chain flexibility*'[58] with values of C_n and L_p as low as 3.0 and 1.9 nm, respectively. However, in the work of Urbani et al.[51] C_n and L_p increased to about 85 and 7 nm, respectively, for the polymer populating all the states in basin b_2 only. The latter result agrees very well with the value of the (intrinsic) persistence length (namely 6.8 nm) of the ordered conformation of κ-carrageenan at infinite ionic strength, extrapolated from experimental light-scattering data obtained as a function of the concentration of the supporting electrolyte.[18] This value has been recently confirmed by a SAXS study of κ-carrageenan solutions.[69] Recent light-scattering experiments at intermediate ionic strength (0.1 M, therefore producing only a moderate electrostatic screening) provide values of L_p of 35.6 (±3.6) nm for the ordered conformation (in aqueous NaI) and still as high as 15.7 (±1.3) nm for the disordered form (in aqueous NaCl),[23] underlining the high stiffness of the chain backbone under all circumstances. It may not be co-incidental that the observed optical activity of the disordered conformation of κ-carrageenan is as high as about two thirds of that of the ordered conformation. This could mean a very high degree of 'residual' order in the former case, to which the definition of 'loose helix'[27] would more appropriately apply, as suggested by Guenet for agarose,[26] the red algal galactan related to carrageenans.

4. Conclusions

Once interference from chain aggregation is eliminated, accurate NMR data can be obtained, and conclusive evidence can be derived therefrom on the so-called 'disordered' conformation of κ-carrageenan. The main conclusion of this analysis is that a combination of NMR experiments carefully carried out under controlled conditions, together with energy landscape analysis of the conformational accessibility to saccharidic residues is extremely useful for depicting the local conformation of the polymer chain. The conformational range assigned to the two sets of glycosidic bonds is limited by the constraints corresponding to the interproton distances from the NOE experiments and by the energy barriers in the conformational maps. The statistically disordered chains seem to explore a rather restricted range of conformational angles, possibly close to the minima, corresponding to 'ordered' helix. In conditions of conformational disorder in dilute solution, no evidence could be raised in favor of interchain interactions that would justify a 'loose' double-helix related to the one allegedly present in solid-state fibers.

A substantial amount of residual order is detected by optical rotation experiments in the so-called 'disordered' form and a comparatively small increase of conforma-

tional ordering upon decrease of temperature. They both find a remarkably simple explanation by the NMR and molecular-mechanics results. In particular, evidence has been produced from NOE data and of ^{1}H chemical shifts in Me_2SO that the disordered κ-carrageenan possesses a rather rigid chain, which can be best identified with a 'loose helix'.[26,27] A realistic picture of the overall chain can be thereafter provided by using suitable statistical weights for the accessible conformations.

Acknowledgements

The authors wish to dedicate this paper to Prof. David A. Brant, with whom they shared a long life of scientific discussions and friendship. They are grateful to Dr. Juraj Bella for his useful contribution in the optimization of the pulse sequences for the selective 1D experiments.

References

1. Wagner, G.; Wütrich, K. *J. Mol. Biol.* **1982**, *155*, 347–366.
2. Brant, D. A. *Quart. Rev. Biophys.* **1976**, *9*, 527–596.
3. Holmbeck, S. M. A.; Petillo, P. A.; Lerner, L. E. *Biochemistry* **1994**, *33*(3), 14246–14255; Almond, A.; Brass, A.; Sheehan, J. K. *Glycobiology* **1998**, *8*, 973–980; Bush, C. A.; Martin-Pastor, M.; Imberty, A. *Annu. Rev. Biophys. Biomol. Struct.* **1999**, *28*, 269–293.
4. Reid, D. S. Ionic polysaccharides. In *Developments in Ionic Polymers—1*; Wilson, A. D., Prosser, H. J., Eds.; Applied Science: London, UK, 1983.
5. Borgstrom, J.; Quist, P. O.; Piculell, L. *Macromolecules* **1996**, *29*, 5926–5933.
6. Chronakis, L. S.; Ramzi, M. *Biomacromolecules* **2002**, *3*, 793–804.
7. Anderson, N. S.; Campbell, J. W.; Harding, M. M.; Rees, D. A.; Samuel, J. W. B. *J. Mol. Biol.* **1969**, *45*, 85–99.
8. Smidsrød, O.; Andresen, I.-L.; Larsen, B.; Painter, T. *Carbohydr. Res.* **1980**, *80*, C11–C16.
9. Grasdalen, H.; Smidsrød, O. *Macromolecules* **1981**, *14*, 1842–1845.
10. Rochas, C.; Rinaudo, M. *Carbohydr. Res.* **1982**, *105*, 227–236.
11. Norton, I. T.; Goodall, D. M.; Morris, E. R.; Rees, D. A. *J. Chem. Soc., Faraday Trans. 1* **1983**, *79*, 2475–2488.
12. Norton, I. T.; Goodall, D. M.; Morris, E. R.; Rees, D. A. *J. Chem. Soc., Faraday Trans. 1* **1983**, *79*, 2489–2500.
13. Smidsrød, O.; Grasdalen, H. *Hydrobiologia* **1984**, *116/117*, 178–186.
14. Paoletti, S.; Smidsrød, O.; Grasdalen, H. *Biopolymers* **1984**, *23*, 1771–1794.
15. Paoletti, S.; Delben, F.; Cesàro, A.; Grasdalen, H. *Macromolecules* **1985**, *18*, 1834–1841.
16. Austen, K. R. J.; Goodall, D. M.; Norton, I. T. *Biopolymers* **1988**, *27*, 139–155.
17. Millane, R. P.; Chandrasekaran, R.; Arnott, S.; Dea, I. C. M. *Carbohydr. Res.* **1988**, *182*, 1–17.
18. Slootmaekers, D.; De Jonghe, C.; Reynaers, H.; Varkevisser, F. A.; Bloys van Treslong, C. J. *Int. J. Biol. Macromol.* **1988**, *10*, 160–168.
19. Cairns, P.; Atkins, E. D. T.; Miles, M. J.; Morris, V. J. *Int. J. Biol. Macromol.* **1991**, *13*, 65–68.
20. Viebke, C.; Borgström, J.; Piculell, L. *Carbohydr. Polym.* **1995**, *27*, 145–154.
21. Bongaerts, K.; Reynaers, H.; Zanetti, F.; Paoletti, S. *Macromolecules* **1999**, *32*, 675–682.
22. Bongaerts, K.; Reynaers, H.; Zanetti, F.; Paoletti, S. *Macromolecules* **1999**, *32*, 683–689.
23. Cuppo, F.; Reynaers, H.; Paoletti, S. *Macromolecules* **2002**, *35*, 539–547.
24. Foord, S. A.; Atkins, E. D. T. *Biopolymers* **1989**, *28*, 1345–1365.
25. Guenet, J.-M.; Brûlet, A.; Rochas, C. *Int. J. Biol. Macromol.* **1993**, *15*, 131–132.
26. Rochas, C.; Brûlet, A.; Guenet, J.-M. *Macromolecules* **1994**, *27*, 3830–3835.
27. Guenet, J.-M. *Trends Polym. Sci.* **1996**, *4*, 6–11.
28. Yarotsky, S. V.; Shaskov, A. S.; Usov, A. I. *Bioorg. Khim.* **1977**, *3*, 1135–1137.
29. Hammer, G. K.; Battacharjee, S. S.; Yaphe, W. *Carbohydr. Res.* **1977**, *54*, C7–C10.
30. Battacharjee, S. S.; Yaphe, W.; Hammer, G. K. *Carbohydr. Res.* **1978**, *60*, C1–C3.
31. Usov, A. I.; Yarotsky, S. V.; Alezandr, S. S. *Biopolymers* **1980**, *19*, 977–990.
32. Rochas, C.; Rinaudo, M.; Vincendon, M. *Biopolymers* **1980**, *19*, 2165–2175.
33. Rochas, C.; Rinaudo, M.; Vincendon, M. *Int. J. Biol. Macromol.* **1983**, *5*, 111–115.
34. Stortz, C. A.; Cerezo, A. S. *Int. J. Biol. Macromol.* **1991**, *13*, 101–104.
35. Ciancia, M.; Matulewicz, M. C.; Stortz, C. A.; Cerezo, A. S. *Int. J. Biol. Macromol.* **1991**, *13*, 337–340.
36. Grasdalen, H.; Smidsrød, O. *Macromolecules* **1981**, *14*, 229–231.
37. Belton, P. S.; Morris, V. J.; Tanner, S. F. *Int. J. Biol. Macromol.* **1985**, *7*, 53–56.
38. Norton, I. T.; Morris, E. R.; Rees, D. A. *Carbohydr. Res.* **1984**, *134*, 89–101.
39. Lamba, D.; Segre, A. L.; Glover, S.; Mackie, W.; Sheldrick, B.; Perez, S. *Carbohydr. Res.* **1990**, *208*, 215–230.
40. Parra, E.; Caro, H. N.; Jimenez-Barbero, J.; Martin Lomas, M.; Bernabe, M. *Carbohydr. Res.* **1990**, *208*, 83–92.
41. Ueda, K.; Saiki, M.; Brady, J. W. *J. Phys. Chem. B* **2001**, *105*, 8629–8638.
42. Martinsen, A.; Skjåk-Bræk, G.; Smidsrød, O.; Zanetti, F.; Paoletti, S. *Carbohydr. Polym.* **1991**, *15*, 171–193.
43. Bodenhausen, J.; Vold, R. L.; Vold, R. R. *J. Magn. Reson.* **1980**, *37*, 93–106.
44. Ernst, R. R.; Bodenhausen, J.; Wokaun, A. In *Principles of Nuclear Magnetic Resonance in One and Two Dimensions*; Clarendon: Oxford, 1987; pp 516–527.
45. Aue, W. P.; Bartholdi, E.; Ernst, R. R. *J. Chem. Phys.* **1976**, *64*, 2229–2246.
46. Hwang, T.-L.; Shaka, A. J. *J. Magn. Reson. Ser. B* **1993**, *102*, 155–165.
47. Kessler, H.; Oschkinat, H.; Griesinger, C.; Bermell, W. *J. Magn. Reson.* **1986**, *70*, 106–133.
48. Sklenař, V.; Feigon, J. *J. Am. Chem. Soc.* **1990**, *112*, 5644–5645.
49. Bax, A.; Davis, D. G. *J. Magn. Reson.* **1985**, *63*, 207–213.
50. Dauber-Osguthorpe, P.; Roberts, V. A.; Osguthorpe, V. J.; Wolff, J.; Genest, M.; Hagler, A. T. *Protein-Struct. Funct. Genet.* **1988**, *4*, 31–47.

51. Urbani, R.; Di Blas, A.; Cesàro, A. *Int. J. Biol. Macromol.* **1993**, *15*, 24–29.
52. Neuhaus, D.; Williamson, M. *The Nuclear Overhauser Effect in Structural and Conformational Analysis*; VCH: New York, 1989.
53. Perico, A.; Mormino, M.; Urbani, R.; Cesàro, A.; Tylianakis, E.; Dais, P.; Brant, D. A. *J. Phys. Chem. B* **1999**, *103*, 8162–8171.
54. Rajamohanan, P. R.; Ganapathy, S.; Ray; Siddharth, S.; Baiger, M. V.; Mashelkar, R. A. *Macromolecules* **1995**, *28*, 2533–2536.
55. Weiss, G. H.; Kiefer, J. E.; Ferretti, J. A. *J. Magn. Reson.* **1992**, *97*, 227–234.
56. Lamba, D.; Glover, S.; Mackie, W.; Rashid, A.; Sheldrick, B.; Pérez, S. *Glycobiology* **1994**, *4*, 151–163.
57. Hemmingsen, L.; Madsen, D. E.; Esbensen, A. L.; Olsenb, L.; Engelsen, S. B. *Carbohydr. Res.* **2004**, *339*, 937–948.
58. Le Questel, J.-Y.; Cros, S.; Mackie, W.; Pérez, S. *Int. J. Biol. Macromol.* **1995**, *17*, 161–175.
59. Ueda, K.; Brady, J. W. *Biopolymers* **1996**, *38*, 461–469.
60. Ueda, K.; Brady, J. W. *Biopolymers* **1997**, *41*, 323–330.
61. Ueda, K.; Ueda, T.; Sato, T.; Nakayama, H.; Brady, J. W. *Carbohydr. Res.* **2004**, *339*, 1953–1960.
62. Arnott, S.; Scott, W. E.; Rees, D. A.; McNab, C. G. A. *J. Mol. Biol.* **1974**, *182*, 1–17.
63. Ueda, K.; Iwama, K.; Nakayama, H. *Bull. Chem. Soc. Jpn.* **2001**, *74*, 2269–2277.
64. Stortz, C. A. *Carbohydr. Res.* **2001**, *337*, 2311–2323.
65. Stortz, C. A.; Cerezo, A. S. *Biopolymers* **2003**, *70*, 227–239.
66. Sicinska, W.; Adams, B.; Lerner, L. *Carbohydr. Res.* **1993**, *242*, 29–51.
67. Jeffrey, G. A. Hydrogen Bonding in Carbohydrates and Hydrate Inclusion Compounds. In *Advances in Enzymology and Related Areas of Molecular Biology*; Meister, A., Ed.; Wiley: New York, 1992; pp 217–254.
68. Bosco, M.; Picotti, F.; Radoicovich, A.; Rizzo, R. *Biopolymers* **2000**, *53*, 272–280.
69. Cuppo, F.; Bongaerts, K.; Evmenenko, G.; Reynaers, H.; Gamini, A.; Paoletti, S., submitted for publication.